Supplement of Atmos. Chem. Phys., 26, 4423–4437, 2026
https://doi.org/10.5194/acp-26-4423-2026-supplement

Atmospheric Chemistry and Physics
Open Access
EGU

Supplement of

Mechanistic insights into marine boundary layer nucleation: synergistic interactions of typical sulfur, iodine, and nitrogen precursors

Jing Li et al.

Correspondence to: An Ning (anning@bit.edu.cn) and Xiuhui Zhang (zhangxiuhui@bit.edu.cn)

Table of Contents

Supplementary Methods

Multi-Step Cluster Conformational Searching Method

The Equations in Atmospheric Cluster Dynamics Code (ACDC)

Surface Electrostatic Potential (ESP) Analysis

Conversion of Formation Rates for Clusters of Different Sizes

Benchmarking and Sensitivity Analysis of Cluster Formation Energies

Figure S1. Lowest Gibbs free energy conformations of $(IA)_x(MSA)_y(DMA)_z$ ($x + y + z \leq 6$, $z \leq x + y$) cluster optimized at the ωB97X-D/6-311++G(3df, 3pd) (for C, H, O, N, and S atoms) + aug-cc-pVTZ-PP (for I atom) level of theory.

Figure S2. ESP-mapped van der Waals (vdW) surface of the $(IA)_3(MSA)_1(DMA)_2$ cluster. The red region is the electron-deficient region, and the blue region is the electron-rich region.

Figure S3. Cluster formation rates J of IA–DMA and MSA–DMA nucleation. The ACDC simulations were performed at the conditions of T = 278 K, CS = 2.0×10^{-3} s^{-1}, [IA] (or [MSA]) = $10^6 – 10^8$ molec. cm^{-3}, and [DMA] = 0.25 pptv.

Figure S4. Cluster formation rates J (cm^{-3} s^{-1}) of the IA–MSA–DMA and IA–MSA–HIO_2 systems under conditions of T = 278 K, CS = 2.0×10^{-3} s^{-1}, [IA] = 10^7 molec. cm^{-3}, [MSA] = $10^6 - 10^8$ molec. cm^{-3}, [DMA] = 0.25 pptv, and [HIO_2] = 2.0×10^5 molec. cm^{-3}.

Figure S5. Cluster formation rates J (cm^{-3} s^{-1}) of the IA–SA–DMA and IA–MSA–DMA systems as a function of [SA] or [MSA] at **(a)** 278 and **(b)** 248 K. Key fixed conditions: [IA] = 10^7 molec. cm^{-3}, [DMA] = 0.25 pptv, CS = 2.0×10^{-3} s^{-1}.

Figure S6. (a) Cluster formation rate J as a function of IA concentration ([IA] = $10^6 – 10^8$ molec. cm^{-3}) under different Gibbs free energy values: ΔG_{278K} (black line), ΔG_{278K} + 0.2 (blue line), and ΔG_{278K} – 0.2 (red line). Conditions: T = 278 K, CS = 2.0×10^{-3} s^{-1}, [MSA] = 10^7 molec. cm^{-3}, and [DMA] = 0.25 pptv. **(b)** J for the IA–MSA–DMA system under different sticking factor (SF)

conditions.

Figure S7. Three-dimensional response surface of the nucleation rate to precursor concentrations. **(a)** Full 3D surface showing the joint dependence on IA, MSA, and DMA. **(b–d)** Two-dimensional projections with one precursor concentration held constant, demonstrating sensitivity to the other two: **(b)** fixed [IA], **(c)** fixed [MSA], and **(d)** fixed [DMA].

Figure S8. The simulated primary cluster growth pathways of IA–MSA–DMA system at the simulation conditions of T = 288 – 298 K, CS = 2.0 × 10^{-3} s^{-1}, [IA] = 10^7 molec. cm^{-3}, [MSA] = 10^7 molec. cm^{-3}, and [DMA] = 0.25 pptv.

Figure S9. Cluster formation rates of the IA–MSA–DMA system under different energy conditions. Common conditions: T = 278 K, CS = 2.0 × 10^{-3} s^{-1}, [IA] = 10^6 – 10^8 molec. cm^{-3}, [MSA] = 10^7 molec. cm^{-3}, and [DMA] = 0.25 pptv. $J_{(1)}$ represents the baseline formation rate using our original calculated Gibbs free energies. $J_{(2)}$ tests the sensitivity by applying the following energy corrections: +1.68 kcal mol^{-1} to the $(IA)_1(DMA)_1$ cluster, +0.17 kcal mol^{-1} to the $(IA)_1(MSA)_1$ cluster, and -0.98 kcal mol^{-1} to the $(IA)_1(MSA)_1(DMA)_1$ cluster.

Table S1. The Gibbs formation free energies ΔG_{ref} (kcal mol^{-1}) of the studied IA–MSA–DMA clusters at the DLPNO-CCSD(T)/aug-cc-pVTZ(-PP)//ωB97X-D/6-311++G(3df,3pd) (for C, H, O, N, and S atoms) + aug-cc-pVTZ-PP with ECP28MDF (for I atom) level of theory, P = 1 atm, and T = 258, 268, 278, 288, and 298 K.

Table S2. The total evaporation rate coefficients ($\Sigma\gamma$, s^{-1}) of IA–MSA–DMA clusters calculated at 268 – 288 K.

Table S3. Boundary conditions of the ACDC simulations at 258 – 298 K, respectively.

Table S4. Cartesian coordinates of all IA–MSA–DMA clusters in the present study at the ωB97X-D/6-311++G(3df,3pd) (for C, H, O, N, and S atoms) + aug-cc-pVTZ-PP with ECP28MDF (for I atom) level of theory.

Table S5. Comparison of single-point electronic energies (in kcal mol^{-1}) for selected clusters.

Supplementary Methods

Multi-Step Cluster Conformational Searching Method

Initially, the artificial bee colony algorithm combined with UFF force field (Rappé et al., 1992) was utilized via ABCluster (Zhang and Dolg, 2015) to generate over 5000 configurations for each cluster. Subsequently, up to 1000 relatively low-energy structures were selected and subjected to optimize at the PM7 semi-empirical method (Stewart, 2013) using MOPAC 2016 (Stewart, 2016). Following this step, approximately 100 of the lowest-energy configurations were re-optimized at the ωB97X-D/6-31+G* (for C, H, O, N, and S atoms) + Lanl2DZ (for I atom) level of theory (Elm and Kristensen, 2017), based on the proven accuracy of the ωB97X-D functional in studying atmospheric clusters. Finally, the 10 most stable isomers were further optimized at a higher level of theory: ωB97X-D/6-311++G(3df,3pd) (for C, H, O, N, and S atoms) + aug-cc-pVTZ-PP with ECP28MDF (for I atom) (Francl et al., 1982; Peterson et al., 2003), to identify the global minimum structure.

The Equations in Atmospheric Cluster Dynamics Code (ACDC)

The birth-death equation (Eq. (S1)) of IA–MSA–DMA system as following:

$$\frac{d_{C_i}}{dt} = \frac{1}{2}\sum_{j<i}\beta_{j,(i-j)}C_jC_{(i-j)} + \sum_j \gamma_{(i+j)\to i}C_{i+j} - \sum_j \beta_{i,j}C_iC_j - \frac{1}{2}\sum_{j<i}\gamma_{i\to j}C_i + Q_i - S_i \quad \text{(S1)}$$

where C_i refers to the concentration of cluster i (where i denotes the cluster index). $\beta_{i,j}$ represents the collision rate coefficient between clusters i and j, while $\gamma_{(i+j)\to i}$ describes evaporation rate constant for the decomposition of cluster $(i + j)$ into smaller clusters i and j. Q_i and S_i denote the external source and possible loss term of cluster i, respectively.

The collision rate coefficient between clusters i and j ($\beta_{i,j}$) is obtained based on the kinetic gas theory, which is given as:

$$\beta_{i,j} = \left(\frac{3}{4\pi}\right)^{1/6}\left(\frac{6k_BT}{m_i} + \frac{6k_BT}{m_j}\right)^{1/2}\left(V_i^{1/3} + V_j^{1/3}\right)^2 \quad \text{(S2)}$$

where m_i and V_i are the mass and volume of cluster i, respectively. Equation (S2) is derived from the hard-sphere collision theory where the volume of molecule clusters $V_i = 3/4 \times \pi \times (d_i/2)^3$. The diameter d_i of cluster i is derived from the cluster volume V_i calculated by Multiwfn 3.7 (Lu and Chen, 2012). Evaporation rate coefficient $\gamma_{(i+j)\to i}$ is derived from the collision coefficients based on the detailed balance assumption:

$$\gamma_{(i+j)\to i} = \beta_{i,j}\frac{P_{\text{ref}}}{k_BT}\exp\left(\frac{\Delta G_{i+j} - \Delta G_i - \Delta G_j}{k_BT}\right) \quad \text{(S3)}$$

where P_{ref} is the reference pressure (1 atm) and ΔG_i is the Gibbs free energy of the formation of cluster i.

Surface Electrostatic Potential (ESP) Analysis

The molecular electrostatic potential (ESP) analysis can provide insights into the reactive sites of the nucleation precursors. As shown in Fig.1, the MSA molecule exhibits a pronounced ESP maximum (+63.95 kcal mol^{-1}) at the hydrogen atom of the –OH group, indicating strong electrophilic character and suggesting its potential as a hydrogen bond (HB) donor. Further analysis reveals two ESP minima (-29.46 and -32.10 kcal mol^{-1}) located at the terminal O atoms of the –SO_3H group, indicating nucleophilic regions capable of acting as HB or halogen bond (XB) acceptors. Similarly, the DMA molecule displays an ESP minimum (-34.38 kcal mol^{-1}) at the N atom of the –NH group, making it a potential acceptor site for HB or XB interactions. In addition, the H atom within the –NH group presents an ESP maximum (+25.79 kcal mol^{-1}), indicating its potential as a HB donor. For the IA molecule, a significant ESP maximum (+59.09 kcal mol^{-1}) is located at the H atom of the –OH group, allowing it to serve as an HB donor. Moreover, an ESP maximum (+51.90 kcal mol^{-1}) is identified along the O–I direction, highlighting its capacity to function as a HB donor. The terminal O atoms of the IA molecule exhibit two ESP minima (-29.10 and -29.47 kcal mol^{-1}), suggesting that these sites can act as HB or XB acceptors. These ESP-based observations collectively indicate that IA, MSA, and DMA molecules possess complementary electrostatic features that facilitate the formation of stable molecular clusters via hydrogen and/or halogen bonding. For instance, Fig. 1(d) illustrates the optimized structure of $(IA)_2(MSA)_1(DMA)_1$ cluster, where blue dashed lines denote HBs and red dashed lines represent XBs, further confirming the critical role of intermolecular interactions in stabilizing cluster formation.

Conversion of Formation Rates for Clusters of Different Sizes

Regarding the difference between simulated formation rates and experimentally reported nucleation rates, we note that particle formation rates are typically reported at a larger size (e.g., 1.5 nm), whereas our simulations track the formation of clusters at 1.2 nm. During the growth from 1.2 to 1.5 nm, clusters may be lost due to coagulation or scavenging by preexisting particles. According to the Kerminen–Kulmala equation (Kulmala et al., 2012), the relationship between formation rates at different sizes can be estimated by considering the growth rate and condensation sink, in which cluster formation rates for d_2 nm clusters (J_{d_2}) relate to those for larger diameter d_1 nm clusters (J_{d_1}) by

$$J_{d_1} = J_{d_2} \exp\left\{\gamma\left(\frac{1}{d_1}-\frac{1}{d_2}\right)\frac{\mathrm{CS}'}{\mathrm{GR}_{d_1-d_2}}\right\} \quad \text{(S4)}$$

where the parameter γ depends on many factors but can usually be approximated by assuming it to be equal to 0.23 $nm^2\ m^2\ h^{-1}$. The $GR_{d_2\text{-}d_1}$ is the initial cluster growth rate from d_2 to d_1 nm, and CS' represents condensation sink of clusters by preexisting particles. GR was measured to be 3.2 – 4.4 $nm \cdot h^{-1}$ in the 1.1 – 2.0 nm size range during three observed events (Xia et al., 2020; Yu et al., 2019). According to the study of Kerminena and Kulmalab (2002), we have converted the CS value to CS' by the following equation (Kerminen and Kulmala, 2002):

$$\mathrm{CS} = 4\pi \mathrm{D}_i \mathrm{CS}' \quad \text{(S5)}$$

where D_i is the diffusion coefficient of the condensing vapor, usually assumed to be sulfuric acid (0.08 $cm^{-2}\ s^{-1}$) (Kulmala et al., 2012).

Benchmarking and Sensitivity Analysis of Cluster Formation Energies

To assess the accuracy of our computational protocol, we performed benchmark tests against higher-level theoretical methods. Taking the ZORA-CCSD(T)/TZVPP level of theory used in Engsvang et al. (2024) as the reference, our calculated binding energies show varying deviations depending on the cluster composition (Table S5). For the $(IA)_1(DMA)_1$ dimer, the deviation reaches 1.68 kcal mol^{-1}, which exceeds the conventional threshold for chemical accuracy (1 kcal mol^{-1}). However, the benchmark tests also reveal that the binding energy for $(IA)_1(MSA)_1$ is overestimated by only 0.17 kcal mol^{-1}, while that for $(IA)_1(MSA)_1(DMA)_1$ is actually underestimated by 0.98 kcal mol^{-1}. Although larger clusters were not benchmarked due to the high computational cost of the ZORA-CCSD(T) calculations (Lesiuk, 2022; Khatun et al., 2023), these available results suggest a cluster-dependent error pattern rather than a consistent bias toward over-stabilization of the entire IA–MSA–DMA pathway. Moreover, Schmitz and Elm (2020) showed that the DLPNO-CCSD(T)/aug-cc-pVTZ(-PP) level of theory employed in our work can yield both overestimations and underestimations, but still produces RMSD values within 1 kcal mol^{-1} for the tested cluster formation energies, thereby supporting the overall accuracy of this method. In addition, this level of theory has been successfully applied in other studies of iodine-containing nucleation systems(Ma et al., 2023; He et al., 2023).

To further assess whether the 1.68 kcal mol^{-1} overestimation in the $(IA)_1(DMA)_1$ cluster binding energy could substantially bias the predicted nucleation rates, we performed an additional sensitivity analysis by correcting the energies of the three benchmarked clusters relative to our original results and recalculating the corresponding formation rates. The results show that although such energy corrections can substantially affect individual evaporation rates, for instance by changing the $(IA)_1(DMA)_1$ cluster evaporation rate by about one order of magnitude, the overall nucleation rate is affected to a much smaller extent (Fig. S9). This behavior likely reflects partial error cancellation, since the benchmark tests indicate both overestimations and underestimations for different clusters rather than a uniform systematic bias.

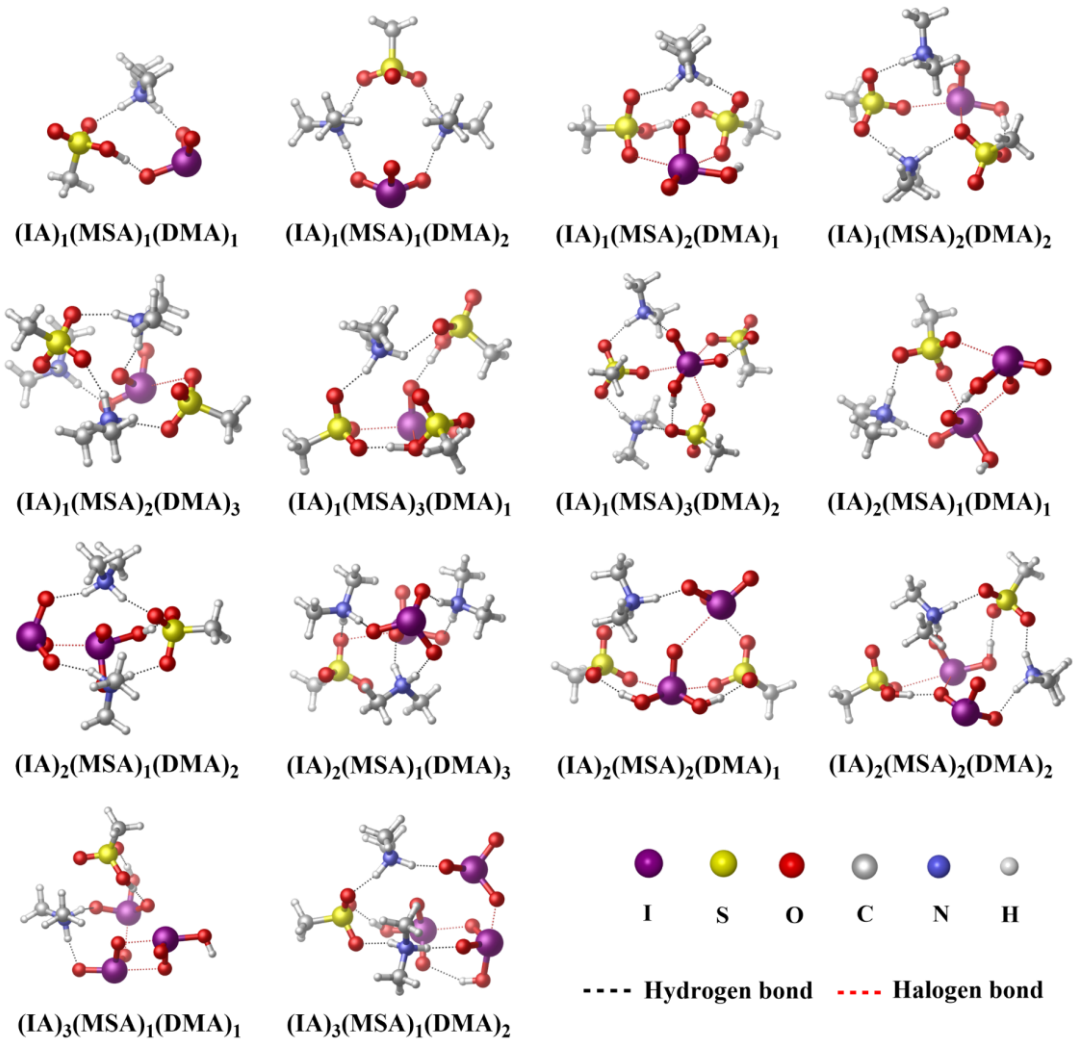

Figure S1. Lowest Gibbs free energy conformations of $(IA)_x(MSA)_y(DMA)_z$ ($x + y + z \leq 6$, $z \leq x + y$) cluster optimized at the ωB97X-D/6-311++G(3df, 3pd) (for C, H, O, N, and S atoms) + aug-cc-pVTZ-PP (for I atom) level of theory.

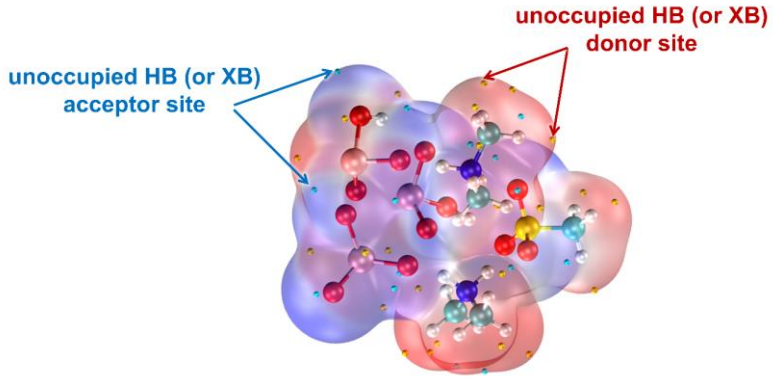

Figure S2. ESP-mapped van der Waals (vdW) surface of the $(IA)_3(MSA)_1(DMA)_2$ cluster. The red region is the electron-deficient region, and the blue region is the electron-rich region.

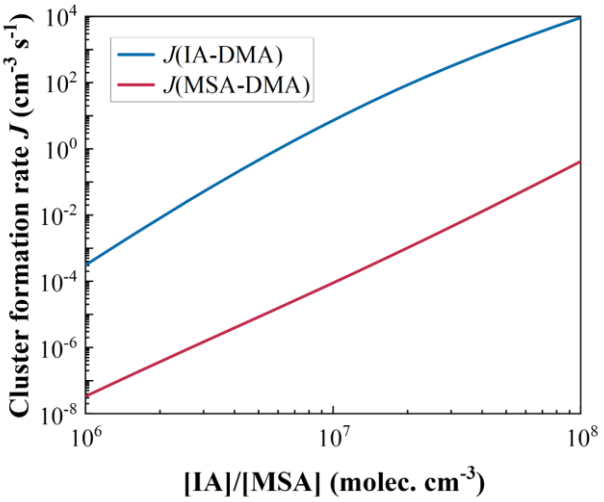

Figure S3. Cluster formation rates J of IA–DMA and MSA–DMA nucleation. The ACDC simulations were performed at the conditions of T = 278 K, CS = 2.0×10^{-3} s^{-1}, [IA] (or [MSA]) = 10^6 – 10^8 molec. cm^{-3}, and [DMA] = 0.25 pptv.

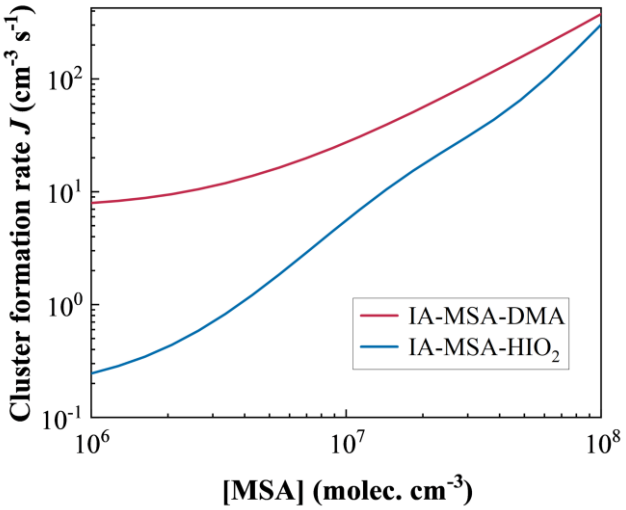

Figure S4. Cluster formation rates J (cm^{-3} s^{-1}) of the IA–MSA–DMA and IA–MSA–HIO_2 systems under conditions of T = 278 K, CS = 2.0×10^{-3} s^{-1}, [IA] = 10^7 molec. cm^{-3}, [MSA] = $10^6 - 10^8$ molec. cm^{-3}, [DMA] = 0.25 pptv, and [HIO_2] = 2.0×10^5 molec. cm^{-3}.

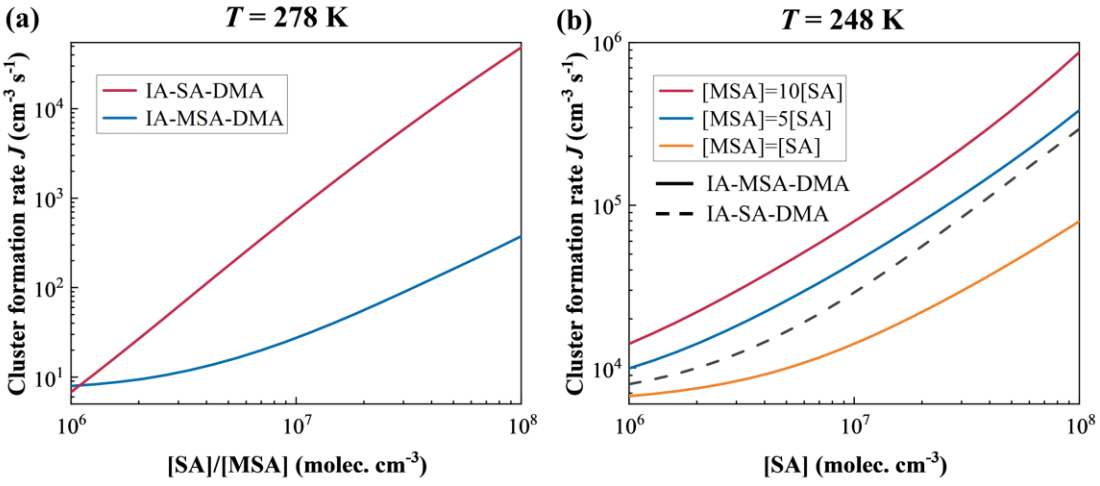

Figure S5. Cluster formation rates J (cm^{-3} s^{-1}) of the IA–SA–DMA and IA–MSA–DMA systems as a function of [SA] or [MSA] at **(a)** 278 and **(b)** 248 K. Key fixed conditions: [IA] = 10^7 molec. cm^{-3}, [DMA] = 0.25 pptv, CS = 2.0×10^{-3} s^{-1}.

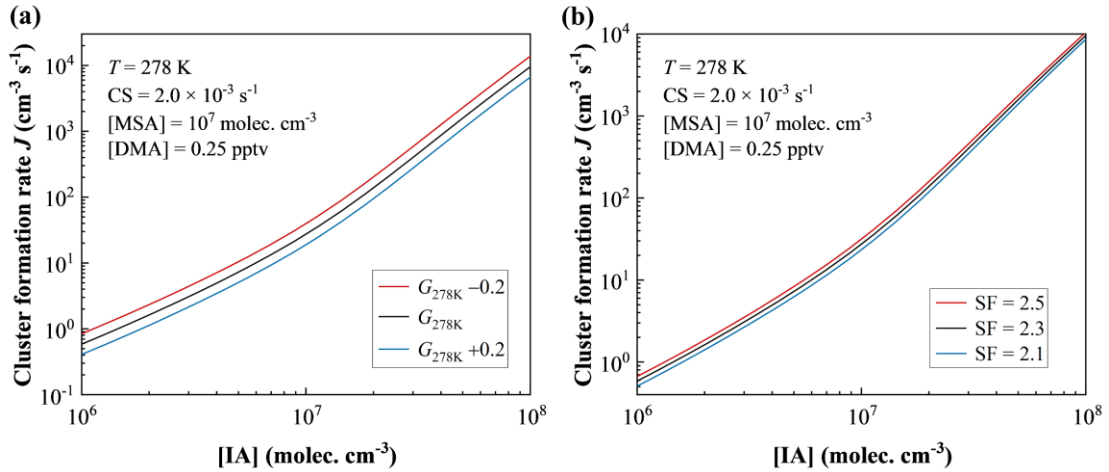

Figure S6. (a) Cluster formation rate J as a function of IA concentration ([IA] = 10^6 – 10^8 molec. cm^{-3}) under different Gibbs free energy values: ΔG_{278K} (black line), ΔG_{278K} + 0.2 (blue line), and ΔG_{278K} – 0.2 (red line). Conditions: T = 278 K, CS = 2.0 × 10^{-3} s^{-1}, [MSA] = 10^7 molec. cm^{-3}, and [DMA] = 0.25 pptv. **(b)** J for the IA–MSA–DMA system under different sticking factor (SF) conditions.

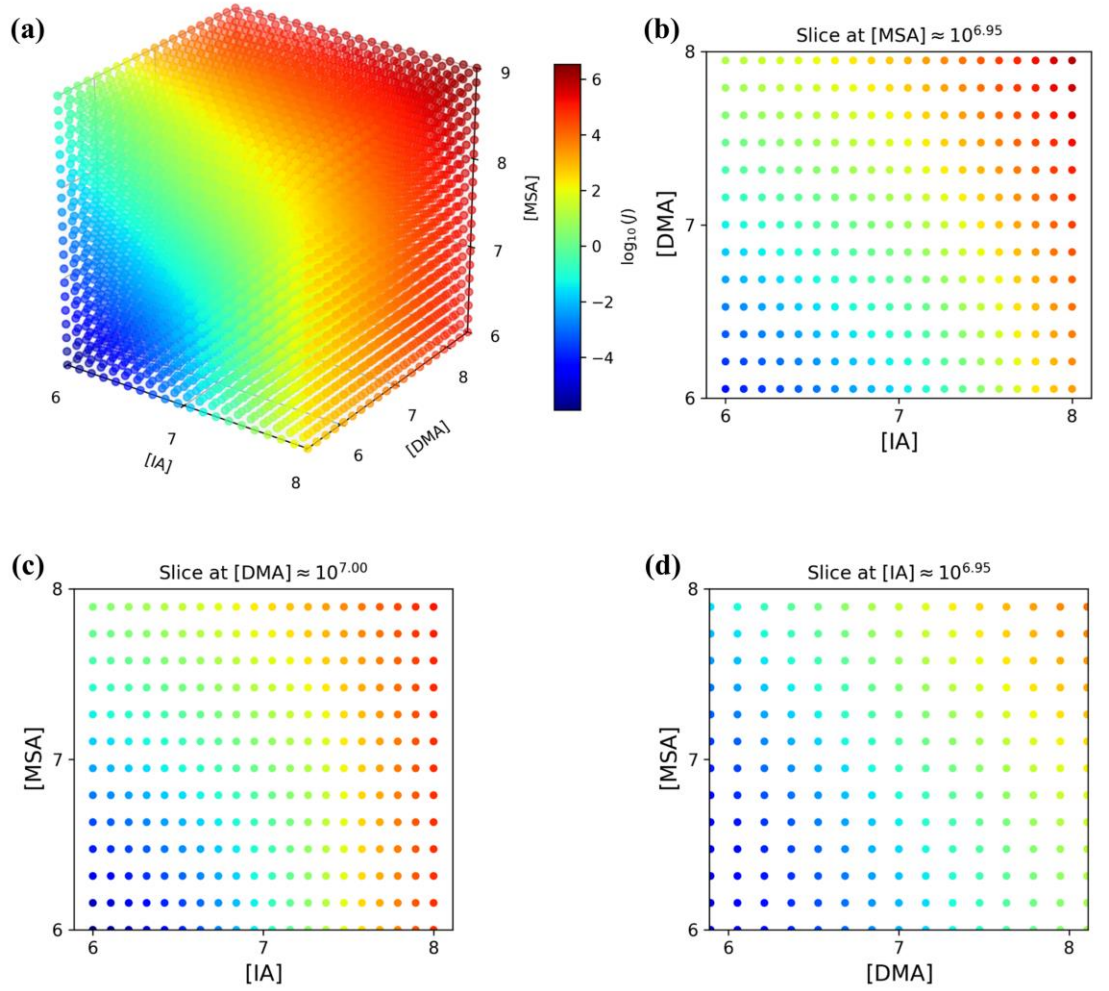

Figure S7. Three-dimensional response surface of the nucleation rate to precursor concentrations. **(a)** Full 3D surface showing the joint dependence on IA, MSA, and DMA. **(b–d)** Two-dimensional projections with one precursor concentration held constant, demonstrating sensitivity to the other two: **(b)** fixed [IA], **(c)** fixed [MSA], and **(d)** fixed [DMA].

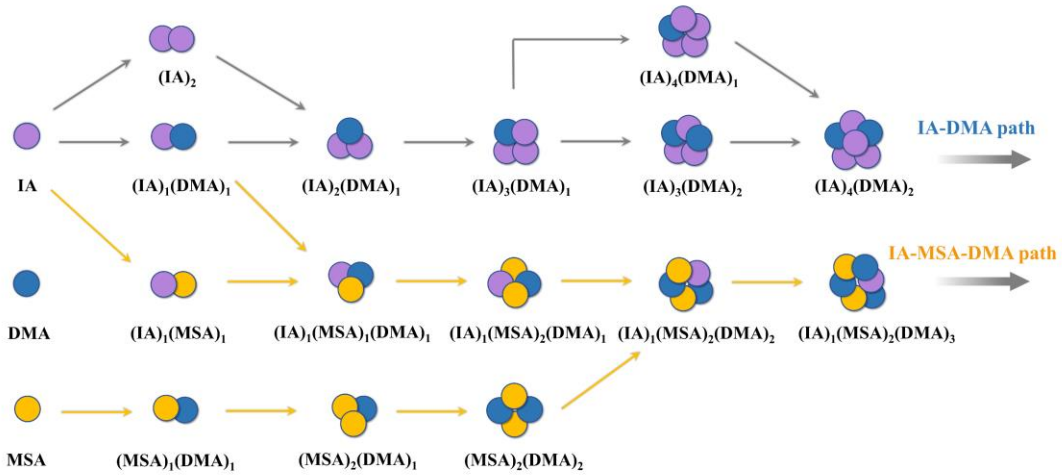

Figure S8. The simulated primary cluster growth pathways of IA–MSA–DMA system at the simulation conditions of T = 288 – 298 K, CS = 2.0 × 10^{-3} s^{-1}, [IA] = 10^7 molec. cm^{-3}, [MSA] = 10^7 molec. cm^{-3}, and [DMA] = 0.25 pptv.

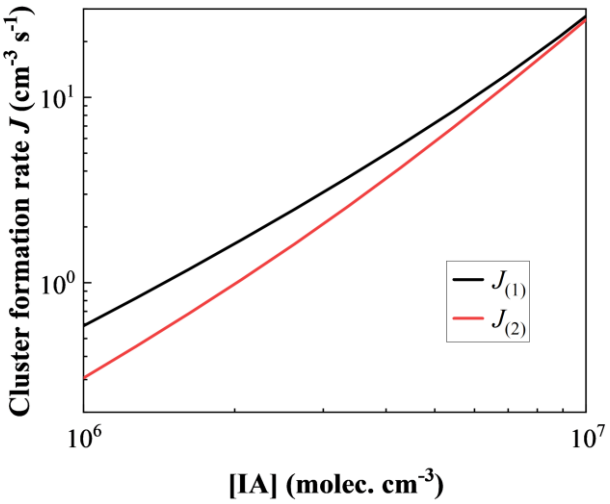

Figure S9. Cluster formation rates of the IA–MSA–DMA system under different energy conditions. Common conditions: T = 278 K, CS = 2.0 × 10^{-3} s^{-1}, [IA] = 10^6 – 10^8 molec. cm^{-3}, [MSA] = 10^7 molec. cm^{-3}, and [DMA] = 0.25 pptv. $J_{(1)}$ represents the baseline formation rate using our original calculated Gibbs free energies. $J_{(2)}$ tests the sensitivity by applying the following energy corrections: +1.68 kcal mol^{-1} to the $(IA)_1(DMA)_1$ cluster, +0.17 kcal mol^{-1} to the $(IA)_1(MSA)_1$ cluster, and -0.98 kcal mol^{-1} to the $(IA)_1(MSA)_1(DMA)_1$ cluster.

Table S1. The Gibbs formation free energies ΔG_{ref} (kcal mol^{-1}) of the studied IA–MSA–DMA clusters at the DLPNO-CCSD(T)/aug-cc-pVTZ(-PP)//ωB97X-D/6-311++G(3df,3pd) (for C, H, O, N, and S atoms) + aug-cc-pVTZ-PP with ECP28MDF (for I atom) level of theory, P = 1 atm, and T = 258, 268, 278, 288, and 298 K.

Clusters	**ΔG (kcal mol^{-1})**				
	258 K	**268 K**	**278 K**	**288 K**	**298 K**
$(IA)_1(MSA)_1$	-12.85	-12.46	-12.07	-11.69	-11.30
$(IA)_1(MSA)_2$	-20.43	-19.65	-18.87	-18.10	-17.33
$(IA)_1(MSA)_3$	-32.12	-30.88	-29.64	-28.41	-27.18
$(IA)_2(MSA)_1$	-24.43	-23.63	-22.83	-22.04	-21.25
$(IA)_2(MSA)_2$	-33.93	-32.70	-31.48	-30.26	-29.04
$(IA)_2(MSA)_3$	-45.25	-43.65	-42.06	-40.47	-38.89
$(IA)_3(MSA)_1$	-34.10	-32.95	-31.80	-30.65	-29.51
$(IA)_3(MSA)_2$	-53.40	-51.80	-50.21	-48.62	-47.04
$(IA)_3(MSA)_3$	-64.94	-62.84	-60.75	-58.67	-56.59
$(IA)_4(MSA)_1$	-57.37	-55.69	-54.01	-52.33	-50.67
$(IA)_4(MSA)_2$	-72.45	-70.36	-68.27	-66.18	-64.11
$(IA)_5(MSA)_1$	-67.40	-65.36	-63.34	-61.31	-59.30
$(MSA)_2$	-9.22	-8.81	-8.41	-8.01	-7.60
$(MSA)_3$	-14.68	-13.89	-13.10	-12.43	-11.66
$(IA)_2$	-12.96	-12.59	-12.22	-11.85	-11.48
$(IA)_3$	-25.35	-24.55	-23.77	-22.98	-22.20
$(IA)_4$	-44.75	-43.52	-42.30	-41.09	-39.88
$(IA)_5$	-61.35	-59.70	-58.06	-56.42	-54.79
$(IA)_6$	-77.14	-75.06	-72.97	-70.90	-68.84
$(IA)_1(DMA)_1$	-11.79	-11.42	-11.04	-10.67	-10.30
$(IA)_1(DMA)_2$	-18.85	-18.12	-17.38	-16.65	-15.92
$(IA)_1(DMA)_3$	-18.91	-17.82	-16.74	-15.67	-14.60
$(IA)_2(DMA)_1$	-32.35	-31.59	-30.83	-30.07	-29.31
$(IA)_2(DMA)_2$	-45.39	-44.29	-43.20	-42.11	-41.02
$(IA)_2(DMA)_3$	-38.85	-37.33	-35.82	-34.32	-32.82
$(IA)_3(DMA)_1$	-46.39	-45.25	-44.11	-42.98	-41.85
$(IA)_3(DMA)_2$	-65.15	-63.56	-61.96	-60.37	-58.79
$(IA)_3(DMA)_3$	-60.92	-58.99	-57.05	-55.13	-53.21

$(IA)_4(DMA)_1$	-61.86	-60.29	-58.72	-57.16	-55.61
$(IA)_4(DMA)_2$	-81.61	-79.60	-77.58	-75.58	-73.58
$(IA)_5(DMA)_1$	-80.97	-78.89	-76.81	-74.73	-72.66
$(DMA)_2$	4.03	4.37	4.71	5.05	5.39
$(DMA)_3$	6.07	6.78	7.49	8.19	8.89
$(MSA)_1(DMA)_1$	-10.37	-9.98	-9.58	-9.19	-8.80
$(MSA)_2(DMA)_1$	-28.16	-27.38	-26.60	-25.82	-25.04
$(MSA)_2(DMA)_2$	-44.56	-43.39	-42.22	-41.05	-39.89
$(MSA)_3(DMA)_1$	-40.01	-38.81	-37.62	-36.43	-35.24
$(MSA)_3(DMA)_2$	-55.65	-54.07	-52.49	-50.91	-49.35
$(MSA)_3(DMA)_3$	-75.22	-73.28	-71.34	-69.41	-67.49
$(IA)_1(MSA)_1(DMA)_1$	-28.28	-27.54	-26.79	-26.05	-25.31
$(IA)_1(MSA)_1(DMA)_2$	-46.29	-45.19	-44.10	-43.01	-41.92
$(IA)_2(MSA)_1(DMA)_1$	-46.49	-45.33	-44.17	-43.01	-41.86
$(IA)_2(MSA)_1(DMA)_2$	-66.27	-64.66	-63.06	-61.45	-59.86
$(IA)_2(MSA)_1(DMA)_3$	-79.76	-77.77	-75.79	-73.81	-71.84
$(IA)_3(MSA)_1(DMA)_1$	-59.06	-57.45	-55.85	-54.25	-52.66
$(IA)_3(MSA)_1(DMA)_2$	-81.40	-79.37	-77.33	-75.31	-73.29
$(IA)_1(MSA)_2(DMA)_1$	-44.03	-42.86	-41.70	-40.54	-39.39
$(IA)_1(MSA)_2(DMA)_2$	-62.26	-60.74	-59.23	-57.73	-56.22
$(IA)_1(MSA)_2(DMA)_3$	-78.95	-76.97	-74.99	-73.01	-71.04
$(IA)_2(MSA)_2(DMA)_1$	-63.22	-61.61	-60.00	-58.40	-56.80
$(IA)_2(MSA)_2(DMA)_2$	-83.35	-81.40	-79.45	-77.50	-75.57
$(IA)_1(MSA)_3(DMA)_1$	-56.10	-54.54	-52.98	-51.42	-49.87
$(IA)_1(MSA)_3(DMA)_2$	-75.92	-73.89	-71.86	-69.84	-67.82

Table S2. The total evaporation rate coefficients ($\Sigma\gamma$, s^{-1}) of IA–MSA–DMA clusters calculated at 268 – 288 K.

Clusters	$\Sigma\gamma$ (s^{-1})		
	268 K	**278 K**	**288 K**
$(IA)_2$	1.80×10^{-1}	8.09×10^{-1}	3.27×10^{0}
$(IA)_3$	1.26×10^{0}	5.83×10^{0}	2.47×10^{1}
$(IA)_4$	2.64×10^{-6}	2.07×10^{-5}	1.36×10^{-4}
$(IA)_5$	5.37×10^{-4}	3.36×10^{-3}	1.88×10^{-2}
$(IA)_6$	2.67×10^{-3}	1.67×10^{-2}	8.87×10^{-2}
$(MSA)_2$	3.44×10^{2}	1.26×10^{3}	4.23×10^{3}
$(MSA)_3$	8.18×10^{5}	2.29×10^{6}	4.85×10^{6}
$(DMA)_2$	2.30×10^{13}	3.12×10^{13}	4.12×10^{13}
$(DMA)_3$	1.28×10^{12}	2.09×10^{12}	3.23×10^{12}
$(IA)_1(MSA)_1$	1.18×10^{0}	5.46×10^{0}	2.22×10^{11}
$(IA)_1(MSA)_2$	1.43×10^{4}	4.63×10^{4}	1.38×10^{5}
$(IA)_1(MSA)_3$	8.23×10^{0}	3.97×10^{1}	1.71×10^{2}
$(IA)_2(MSA)_1$	1.57×10^{1}	6.99×10^{1}	2.78×10^{2}
$(IA)_2(MSA)_2$	4.53×10^{2}	1.76×10^{3}	6.31×10^{3}
$(IA)_2(MSA)_3$	1.51×10^{1}	6.08×10^{1}	2.22×10^{2}
$(IA)_3(MSA)_1$	1.71×10^{3}	5.80×10^{3}	1.78×10^{4}
$(IA)_3(MSA)_2$	7.65×10^{-6}	5.76×10^{-5}	3.77×10^{-4}
$(IA)_3(MSA)_3$	1.32×10^{1}	6.76×10^{1}	3.03×10^{2}
$(IA)_4(MSA)_1$	1.37×10^{0}	7.05×10^{0}	3.28×10^{1}
$(IA)_4(MSA)_2$	1.41×10^{-2}	7.82×10^{-2}	3.85×10^{-1}
$(IA)_5(MSA)_1$	2.99×10^{5}	8.57×10^{5}	2.32×10^{6}
$(IA)_1(DMA)_1$	9.93×10^{0}	4.19×10^{1}	1.57×10^{2}
$(IA)_1(DMA)_2$	4.24×10^{4}	1.26×10^{5}	3.45×10^{5}
$(IA)_1(DMA)_3$	2.48×10^{10}	4.41×10^{10}	7.55×10^{10}
$(IA)_2(DMA)_1$	4.12×10^{-6}	2.97×10^{-5}	1.87×10^{-4}
$(IA)_2(DMA)_2$	6.08×10^{-1}	2.56×10^{0}	9.74×10^{0}
$(IA)_2(DMA)_3$	7.33×10^{15}	9.62×10^{15}	1.22×10^{16}
$(IA)_3(DMA)_1$	5.88×10^{-2}	2.89×10^{-1}	1.25×10^{3}

$(IA)_3(DMA)_2$	1.95×10^{-5}	1.54×10^{-4}	1.05×10^{-3}
$(IA)_3(DMA)_3$	8.78×10^{13}	1.17×10^{14}	1.51×10^{14}
$(IA)_4(DMA)_1$	4.98×10^{-3}	2.94×10^{-2}	1.53×10^{-1}
$(IA)_4(DMA)_2$	7.75×10^{-4}	4.81×10^{-3}	2.59×10^{-2}
$(IA)_5(DMA)_1$	9.85×10^{-6}	8.29×10^{-5}	6.09×10^{-4}
$(MSA)_1(DMA)_1$	1.74×10^{2}	6.90×10^{2}	2.45×10^{3}
$(MSA)_2(DMA)_1$	7.67×10^{-5}	4.90×10^{-4}	2.80×10^{-3}
$(MSA)_2(DMA)_2$	1.15×10^{-3}	6.73×10^{-3}	3.49×10^{-2}
$(MSA)_3(DMA)_1$	5.06×10^{0}	2.26×10^{1}	9.08×10^{1}
$(MSA)_3(DMA)_2$	2.29×10^{1}	9.72×10^{1}	3.73×10^{2}
$(MSA)_3(DMA)_3$	3.34×10^{-6}	2.31×10^{-5}	1.37×10^{-4}
$(IA)_1(MSA)_1(DMA)_1$	7.30×10^{-3}	3.84×10^{-2}	1.81×10^{-1}
$(IA)_1(MSA)_1(DMA)_2$	5.78×10^{-5}	3.46×10^{-4}	1.86×10^{-3}
$(IA)_2(MSA)_1(DMA)_1$	6.79×10^{-2}	3.48×10^{-1}	1.59×10^{0}
$(IA)_2(MSA)_1(DMA)_2$	4.21×10^{-6}	3.58×10^{-5}	2.68×10^{-4}
$(IA)_2(MSA)_1(DMA)_3$	3.42×10^{-1}	1.62×10^{0}	6.77×10^{0}
$(IA)_3(MSA)_1(DMA)_1$	2.48×10^{0}	1.25×10^{1}	5.70×10^{1}
$(IA)_3(MSA)_1(DMA)_2$	1.13×10^{-2}	6.71×10^{-2}	3.36×10^{-1}
$(IA)_1(MSA)_2(DMA)_1$	5.59×10^{-3}	3.20×10^{-2}	1.64×10^{-1}
$(IA)_1(MSA)_2(DMA)_2$	2.70×10^{-3}	1.62×10^{-2}	8.43×10^{-2}
$(IA)_1(MSA)_2(DMA)_3$	9.98×10^{-4}	6.86×10^{-3}	4.20×10^{-2}
$(IA)_2(MSA)_2(DMA)_1$	6.41×10^{-4}	4.27×10^{-3}	2.45×10^{-2}
$(IA)_2(MSA)_2(DMA)_2$	2.90×10^{-4}	1.67×10^{-3}	8.32×10^{-3}
$(IA)_1(MSA)_3(DMA)_1$	3.71×10^{0}	1.65×10^{1}	6.64×10^{1}
$(IA)_1(MSA)_3(DMA)_2$	2.51×10^{-1}	1.54×10^{0}	8.28×10^{0}

Table S3. Boundary conditions of the ACDC simulations at 258 – 298 K, respectively.

Temperature (K)	Boundary cluster
258 K	$(IA)_7$
	$(IA)_6(MSA)_1$
	$(IA)_6(DMA)_1$
	$(IA)_5(MSA)_2$
	$(IA)_5(DMA)_2$
	$(IA)_4(MSA)_3$
	$(IA)_4(DMA)_3$
	$(MSA)_4(DMA)_3$
	$(IA)_4(MSA)_1(DMA)_2$
	$(IA)_5(MSA)_1(DMA)_1$
	$(IA)_1(MSA)_3(DMA)_3$
	$(IA)_2(MSA)_2(DMA)_3$
	$(IA)_3(MSA)_2(DMA)_2$
	$(IA)_2(MSA)_3(DMA)_2$
268 K	$(IA)_7$
	$(IA)_6(DMA)_1$
	$(IA)_5(DMA)_2$
	$(MSA)_4(DMA)_3$
	$(IA)_4(MSA)_1(DMA)_2$
	$(IA)_5(MSA)_1(DMA)_1$
	$(IA)_1(MSA)_3(DMA)_3$
	$(IA)_2(MSA)_2(DMA)_3$
	$(IA)_3(MSA)_2(DMA)_2$
	$(IA)_2(MSA)_3(DMA)_2$
278 K	$(IA)_6(DMA)_1$
	$(IA)_5(DMA)_2$
	$(MSA)_4(DMA)_3$
	$(IA)_5(MSA)_1(DMA)_1$

	$(IA)_1(MSA)_3(DMA)_3$
	$(IA)_3(MSA)_2(DMA)_2$
	$(IA)_2(MSA)_3(DMA)_2$
288 K	$(IA)_6(DMA)_1$
	$(IA)_5(DMA)_2$
	$(MSA)_4(DMA)_3$
	$(IA)_5(MSA)_1(DMA)_1$
	$(IA)_1(MSA)_3(DMA)_3$
298 K	$(IA)_6(DMA)_1$
	$(MSA)_4(DMA)_3$
	$(IA)_5(MSA)_1(DMA)_1$
	$(IA)_1(MSA)_3(DMA)_3$

Table S4. Cartesian coordinates of all IA–MSA–DMA clusters in the present study at the ωB97X-D/6-311++G(3df,3pd) (for C, H, O, N, and S atoms) + aug-cc-pVTZ-PP with ECP28MDF (for I atom) level of theory.

$(IA)_1(MSA)_1(DMA)_1$:

Atoms	X	Y	Z
I	-2.045639	-0.663977	0.097891
O	-1.984089	-0.165251	-1.640758
O	-0.404451	-1.464759	0.394057
O	-1.898779	0.915942	1.026222
H	-0.615576	1.762805	0.511423
N	0.250909	2.249925	0.151151
H	1.045400	1.624169	0.380376
C	0.429770	3.529977	0.854085
H	-0.422702	4.173195	0.649465
H	0.496140	3.339536	1.921556
H	1.344348	4.007563	0.510438
C	0.156781	2.373430	-1.316752
H	-0.020901	1.388806	-1.741471
H	-0.679990	3.021397	-1.565340
H	1.084721	2.789834	-1.701883
C	2.940222	-1.862277	1.047131
H	1.990308	-1.996256	1.559384
H	3.727081	-1.604665	1.750885
H	3.205784	-2.748438	0.477916
S	2.775392	-0.514882	-0.075307
O	3.940248	-0.406072	-0.881841
O	2.401529	0.640833	0.714897
O	1.598302	-0.921800	-0.970786
H	0.718889	-1.116430	-0.435237

$(IA)_1(MSA)_1(DMA)_2$:

Atoms	X	Y	Z
C	4.784265	-0.000222	0.110274
H	5.053507	-0.893429	0.667368
H	5.053734	0.892676	0.667756
H	5.262118	-0.000069	-0.865559
S	3.030786	0.000049	-0.125507
O	2.737714	1.216677	-0.884503
O	2.411760	-0.000111	1.185884
O	2.737386	-1.216234	-0.884931
H	1.289813	-1.896092	-0.364859
N	0.463975	-2.462837	-0.068571
H	-0.405417	-1.989185	-0.417299
C	0.411211	-2.509348	1.403996
H	1.351412	-2.902385	1.782790
H	-0.418235	-3.144137	1.708571
H	0.255343	-1.501434	1.774857
C	0.570817	-3.782878	-0.708338
H	1.466962	-4.284668	-0.350802
H	0.636232	-3.645797	-1.783961
H	-0.309959	-4.373066	-0.466140
N	0.463942	2.462887	-0.068574
H	1.289893	1.896292	-0.364830
C	0.411155	2.509365	1.403993
H	-0.418422	3.143979	1.708576
H	1.351276	2.902586	1.782797
H	0.255483	1.501414	1.774837
C	0.570564	3.782956	-0.708322
H	-0.310320	4.372986	-0.466128
H	0.636012	3.645900	-1.783945
H	1.466619	4.284895	-0.350769
I	-2.594348	-0.000025	-0.061083
O	-1.879450	-1.429732	-0.912654
O	-1.762617	0.000020	1.528978
O	-1.879330	1.429551	-0.912777
H	-0.405367	1.989099	-0.417325

$(IA)_1(MSA)_2(DMA)_1$:

Atoms	X	Y	Z
C	1.450018	-3.413371	-2.049811
H	0.686349	-4.192685	-2.039295
H	2.408893	-3.810552	-1.713246
H	1.539446	-2.974941	-3.045017
S	0.948197	-2.131404	-0.919158
O	2.031497	-1.097932	-0.962853
O	0.858269	-2.752258	0.420795
O	-0.344979	-1.608909	-1.425120
H	-2.102234	-2.048506	-0.548022
C	2.102046	3.816397	-0.925397
H	3.183520	3.730522	-0.816103
H	1.694031	4.539816	-0.217063
H	1.827304	4.081146	-1.947330
S	1.369651	2.247391	-0.538937
O	-0.072905	2.344645	-0.737188
O	1.843702	1.800338	0.770656
O	2.019888	1.368353	-1.674105
H	1.972200	0.374809	-1.441647
N	1.449694	-0.668997	2.209631
H	1.070962	-1.465583	1.658700
C	0.831970	-0.647246	3.554612
H	1.218291	0.212069	4.106075
H	1.085008	-1.572534	4.075780
H	-0.246208	-0.556829	3.422861
C	2.926075	-0.747955	2.205113
H	3.331668	0.139589	2.693100
H	3.255681	-0.790020	1.166816
H	3.233810	-1.650740	2.736498
I	-2.058884	0.310801	-0.065816
O	-2.803040	-1.486529	-0.157863
O	-3.503937	1.117078	0.569188
O	-0.938607	0.080634	1.304417
H	1.148935	0.168888	1.687682

$(IA)_1(MSA)_2(DMA)_2$:

Atoms	X	Y	Z
I	-0.321538	-1.711869	-0.857758
O	-2.080449	-2.455792	-0.765508
O	0.281871	-2.302742	0.731801
O	0.398439	-2.817604	-2.036708
N	1.786793	-0.851436	2.348196
H	2.424702	-0.258401	1.777244
C	2.588575	-1.753775	3.187696
H	1.926498	-2.398318	3.760904
H	3.210893	-1.168195	3.860944
H	3.217927	-2.362390	2.544746
C	0.866739	0.020776	3.097169
H	0.220674	-0.594644	3.719249
H	0.252746	0.566761	2.385199
H	1.440177	0.705632	3.718038
N	-0.218073	2.776825	-0.549695
H	-0.596453	1.981526	0.003063
C	-0.658637	2.587169	-1.944907
H	-0.289366	3.410670	-2.551515
H	-1.744911	2.551741	-1.966112
H	-0.241089	1.651565	-2.306695
C	-0.662212	4.049366	0.047675
H	-0.281067	4.874155	-0.549946
H	-0.260768	4.119394	1.055126
H	-1.747804	4.058100	0.078330
C	3.990940	0.755100	-1.659230
H	3.558292	1.030299	-2.616995
H	4.204002	-0.310077	-1.631152
H	4.889752	1.332917	-1.462468
S	2.813012	1.113512	-0.394828
O	3.440668	0.738557	0.867273
O	1.626127	0.308365	-0.679960
O	2.522281	2.540064	-0.489265
H	0.819284	2.712101	-0.511732
C	-3.655493	0.505973	2.078859
H	-4.728772	0.632617	1.965822
H	-3.263948	1.217796	2.800519
H	-3.422139	-0.514048	2.373168
S	-2.906029	0.821466	0.508585
O	-1.454039	0.621156	0.717219
O	-3.210869	2.187737	0.152871
O	-3.445851	-0.172140	-0.407799
H	-2.700751	-1.699877	-0.619288
I	1.215952	-1.416093	1.662139

$(IA)_1(MSA)_2(DMA)_3$:

Atoms	X	Y	Z
N	-2.667806	1.915634	-0.497422
H	-2.602864	0.886727	-0.593359
C	-3.757793	2.388381	-1.360994
H	-3.856239	3.466633	-1.260254
H	-4.685631	1.900388	-1.071651
H	-3.525230	2.139911	-2.392956
C	-2.855846	2.225930	0.931787
H	-2.981958	3.299502	1.049781
H	-1.966589	1.909294	1.468351
H	-3.726517	1.690748	1.302490
N	0.064638	-1.015223	2.268811
H	-0.966865	-1.040213	2.224535
C	0.529266	-0.080924	3.310770
H	1.615659	-0.064681	3.292021
H	0.165045	-0.415565	4.279942
H	0.164627	0.916488	3.076815
C	0.588511	-2.384164	2.414938
H	1.668208	-2.358607	2.308783
H	0.164662	-2.997086	1.625781
H	0.299892	-2.770161	3.390991
I	0.879404	1.985822	-0.081099
O	-0.018700	0.401938	-0.023671
O	-0.260712	2.862867	-1.199889
O	0.501457	2.671756	1.531018
N	0.296231	-1.573319	-2.001856
H	-0.243944	-1.662403	-1.127633
C	0.643635	-2.925249	-2.468784
H	1.174731	-2.851131	-3.415000
H	-0.270014	-3.501341	-2.592370
H	1.284921	-3.380861	-1.719784
C	-0.506763	-0.784045	-2.950310
H	0.028330	-0.704128	-3.893791
H	-0.660237	0.201477	-2.521030
H	-1.467219	-1.272209	-3.095181
C	-4.031766	-2.930195	0.361375
H	-4.951291	-2.424630	0.643354
H	-3.752575	-3.661224	1.115072
H	-4.140768	-3.406034	-0.609382
S	-2.741709	-1.723846	0.255701
O	-1.533290	-2.462689	-0.097728
O	-2.660717	-1.106893	1.574805
O	-3.154234	-0.788716	-0.786964

H	-1.741130	2.321410	-0.817376
C	4.888209	-0.989146	-0.243124
H	5.254771	-1.405224	0.691581
H	5.289900	0.008427	-0.398301
H	5.145400	-1.639334	-1.074918
S	3.124420	-0.877875	-0.143352
O	2.837203	0.011242	0.975555
O	2.625371	-2.228144	0.040873
O	2.693443	-0.305887	-1.428945
H	1.168046	-1.055486	-1.766119
H	0.308359	-0.608709	1.339129

$(IA)_1(MSA)_3(DMA)_1$:

Atoms	X	Y	Z
I	-0.439023	-2.022909	-0.362748
O	-0.030309	-3.182537	-1.627210
O	0.484720	-0.526190	-0.753054
O	0.749991	-2.684820	1.004612
H	0.838166	-1.991143	1.688201
N	0.250629	2.348767	-1.104139
H	0.813620	1.734426	-0.510215
C	0.586245	2.084855	-2.516848
H	-0.034523	2.716242	-3.147143
H	1.639826	2.297222	-2.673843
H	0.382108	1.038759	-2.722016
C	0.479082	3.743127	-0.684592
H	-0.146068	4.397173	-1.287292
H	0.215795	3.831844	0.364524
H	1.529966	3.979301	-0.825536
C	3.858985	-0.293945	0.988109
H	2.861802	-0.461469	1.387164
H	4.382936	-1.228644	0.811633
H	4.427966	0.346400	1.657478
S	3.713979	0.563898	-0.541114
O	2.846393	1.691934	-0.324638
O	5.003331	0.788177	-1.092311
O	2.991680	-0.456810	-1.463122
H	2.026949	-0.553929	-1.217398
C	-0.799102	0.967495	4.135827
H	0.007301	1.536948	4.590758
H	-1.692223	1.579088	4.039011
H	-1.001012	0.064580	4.704519
S	-0.266734	0.505317	2.523771
O	-0.086195	1.692580	1.748847
O	0.847669	-0.394209	2.668458
O	-1.428650	-0.334713	1.977680
H	-2.211084	0.196269	1.454605
C	-4.812301	0.871154	-1.264898
H	-4.800223	0.901970	-2.350935
H	-5.351001	-0.002957	-0.910760
H	-5.242674	1.782477	-0.859668
S	-3.143021	0.753616	-0.716104
O	-3.237796	0.739627	0.762144
O	-2.607298	-0.492749	-1.233916
O	-2.460339	1.938326	-1.201714
H	-0.745121	2.104485	-0.962685

$(IA)_1(MSA)_3(DMA)_2$:

Atoms	X	Y	Z
I	-0.752924	0.016707	-1.004936
O	0.628388	-0.319461	-2.273488
O	-1.129393	1.688856	-1.540338
O	-2.046621	-0.931075	-1.812624
N	-0.931910	3.599522	0.350141
H	0.091855	3.777829	0.418798
C	-1.408261	3.054033	1.635469
H	-0.773297	2.213620	1.900574
H	-2.432635	2.708511	1.526270
H	-1.341682	3.824600	2.400025
C	-1.645432	4.804349	-0.099010
H	-2.697989	4.568668	-0.235947
H	-1.221194	5.133760	-1.043358
H	-1.537560	5.590106	0.645190
N	3.424126	-0.614839	1.356789
H	2.934361	-1.003639	0.529178
C	2.543513	-0.736287	2.536716
H	3.044243	-0.295813	3.395743
H	2.332446	-1.788361	2.705805
H	1.625840	-0.196806	2.324513
C	4.707636	-1.324639	1.495763
H	4.503365	-2.383980	1.629439
H	5.246783	-0.928336	2.352740
H	5.290278	-1.173149	0.591454
C	2.516531	2.350351	-1.641769
H	1.554116	2.514681	-2.120709
H	2.901119	1.374422	-1.924759
H	3.224500	3.133378	-1.898934
S	2.279158	2.374744	0.108474
O	3.566061	2.054251	0.711961
O	1.276725	1.342753	0.399690
O	1.799083	3.710178	0.439783
H	-1.019222	2.850608	-0.383229
C	1.206204	-4.204288	-1.412062
H	2.184632	-4.591166	-1.682716
H	0.712964	-3.758362	-2.272149
H	0.588696	-4.990419	-0.985982
S	1.416176	-2.953109	-0.184444
O	2.100707	-3.534187	0.942523
O	0.083925	-2.437577	0.107661
O	2.239126	-1.900364	-0.836123
H	1.298316	-0.897607	-1.826494

C	-3.000644	-2.358527	1.651315
H	-3.758599	-3.133967	1.587951
H	-2.708068	-2.194696	2.685376
H	-2.128998	-2.601037	1.044971
S	-3.707353	-0.855125	1.068620
O	-4.137388	-1.183223	-0.373277
O	-2.643109	0.128777	1.018743
O	-4.864087	-0.544529	1.831118
H	3.575544	0.394398	1.151404
H	-3.342655	-1.094764	-1.008035

$(IA)_2(MSA)_1(DMA)_1$:

Atoms	X	Y	Z
I	2.761771	0.368019	0.237782
O	4.324157	-0.421807	0.496584
O	1.833889	-0.691394	-0.881078
O	1.895409	-0.088276	1.878847
H	0.972199	-0.364256	1.647373
I	-0.739574	-1.447543	-0.651879
O	-2.522805	-1.658818	-0.658947
O	-0.519855	-0.923721	1.053180
O	-0.242794	-3.296341	-0.360885
H	-0.338229	-3.500459	0.576488
N	-3.478191	0.297249	0.996313
H	-3.154196	-0.475850	0.368795
C	-4.785580	0.783638	0.528755
H	-5.097860	1.627392	1.139498
H	-5.518506	-0.016596	0.598221
H	-4.684407	1.098078	-0.506139
C	-3.454585	-0.172491	2.392038
H	-3.710954	0.650528	3.054958
H	-2.450976	-0.528810	2.605692
H	-4.171215	-0.982030	2.510855
C	-0.947596	3.449415	-1.625338
H	-1.959193	3.456136	-2.021029
H	-0.225875	3.278116	-2.419078
H	-0.732594	4.379867	-1.106639
S	-0.805584	2.133619	-0.457054
O	0.565476	2.128144	0.001634
O	-1.167639	0.920301	-1.219728
O	-1.785818	2.399982	0.588279
H	-2.781537	1.066119	0.880972

$(IA)_2(MSA)_1(DMA)_2$:

Atoms	X	Y	Z
N	0.548707	-0.147391	2.484557
H	1.338937	-0.419477	1.869758
C	0.197042	-1.261115	3.382245
H	-0.639572	-0.957753	4.007190
H	1.059210	-1.504867	3.998763
H	-0.078038	-2.112627	2.766186
C	0.931233	1.092794	3.180259
H	0.065365	1.483019	3.709026
H	1.280434	1.805510	2.438164
H	1.738102	0.875470	3.875863
N	0.558663	2.378289	-1.251472
H	-0.356290	1.931532	-1.043385
C	0.995131	1.984479	-2.602309
H	1.933333	2.484032	-2.831294
H	0.230516	2.264337	-3.323073
H	1.156002	0.911329	-2.603184
C	0.422704	3.829765	-1.063113
H	1.390526	4.304309	-1.205696
H	0.063839	4.017145	-0.055162
H	-0.298354	4.218371	-1.778063
I	-2.906558	0.647551	0.211062
O	-2.118663	1.831714	-0.898689
O	-2.554349	-0.992833	-0.493503
O	-1.951194	0.726956	1.735761
H	1.262066	2.006082	-0.580349
I	-0.219839	-1.823693	-0.903737
O	0.178224	-0.150108	-0.408314
O	1.486343	-2.201934	-1.705345
O	-0.136834	-2.768991	0.599243
C	5.077523	0.721294	0.411171
H	5.406161	1.398346	-0.372524
H	5.603418	-0.226915	0.341735
H	5.223459	1.170049	1.389856
S	3.351520	0.405496	0.190653
O	2.695337	1.712378	0.313630
O	2.974748	-0.506955	1.261047
O	3.216278	-0.169769	-1.139828
H	2.151060	-1.527068	-1.421624
H	-0.267958	0.063492	1.886010

$(IA)_2(MSA)_1(DMA)_3$:

Atoms	X	Y	Z
N	-2.143149	2.470538	0.055856
H	-1.205410	2.638053	0.513216
C	-3.208167	2.543603	1.067110
H	-4.172809	2.409319	0.582777
H	-3.168983	3.512810	1.558929
H	-3.055986	1.744381	1.788197
C	-2.288571	3.426916	-1.056180
H	-3.188963	3.187118	-1.617348
H	-1.405628	3.343750	-1.686667
H	-2.355452	4.434098	-0.650824
N	0.044268	-0.946387	2.249003
H	0.378864	-0.557745	1.335744
C	0.490199	-2.336595	2.433466
H	0.088069	-2.719578	3.369891
H	1.575397	-2.360205	2.434686
H	0.122357	-2.922723	1.596004
C	0.470797	-0.019434	3.310293
H	0.026985	-0.321735	4.256595
H	0.143930	0.984425	3.045636
H	1.555441	-0.041841	3.370052
I	-2.925572	-1.431857	-0.067825
O	-1.383131	-2.284881	-0.454558
O	-2.669968	-0.819004	1.616464
O	-2.905094	0.060848	-1.080133
I	1.322278	1.928194	-0.085169
O	0.303389	0.422598	-0.017330
O	0.876521	2.554641	-1.706286
O	0.325344	2.953561	1.043552
N	0.718240	-1.422020	-2.077247
H	1.569373	-0.983118	-1.676939
C	0.144212	-0.534031	-3.104320
H	-0.800036	-0.952110	-3.445274
H	0.843556	-0.455295	-3.933486
H	-0.014729	0.445503	-2.662079
C	1.044541	-2.777440	-2.549001
H	0.129847	-3.271157	-2.867591
H	1.503754	-3.315424	-1.724918
H	1.744612	-2.708349	-3.378532
C	5.101623	-1.291447	0.244790
H	5.356359	-1.844761	1.144851
H	5.571148	-0.311624	0.254695
H	5.396659	-1.847282	-0.641078

S	3.344768	-1.073528	0.209820
O	3.073202	-0.315623	-1.024766
O	3.005293	-0.310802	1.402986
O	2.755202	-2.397852	0.171732
H	-2.142967	1.510344	-0.336403
H	-0.986457	-0.918108	2.139948
H	0.040002	-1.500400	-1.301994

$(IA)_2(MSA)_2(DMA)_1$:

Atoms	X	Y	Z
I	0.843747	-1.600292	-0.537454
O	2.159299	-1.360282	-1.879691
O	0.281397	0.071619	-0.353667
O	-0.268386	-2.167803	-1.960057
H	-1.212546	-2.143538	-1.651519
I	-2.277751	1.603808	-0.146995
O	-1.675641	1.555022	1.684090
O	-3.839027	2.419587	-0.006925
O	-1.130784	2.888072	-0.654459
H	0.474713	2.690815	-0.287816
N	1.511144	2.779700	-0.184622
H	1.860135	2.034701	0.433945
C	1.816880	4.077191	0.442392
H	1.456230	4.875104	-0.201630
H	2.891129	4.160530	0.585647
H	1.311492	4.127789	1.402336
C	2.126762	2.593006	-1.512540
H	1.804906	3.399292	-2.166848
H	1.794007	1.638644	-1.909349
H	3.208164	2.586006	-1.406751
C	-3.375837	-3.433562	1.173283
H	-3.200487	-3.549155	2.239124
H	-3.043219	-4.312225	0.628116
H	-4.425619	-3.232810	0.977234
S	-2.453115	-2.045846	0.605953
O	-2.673201	-1.930754	-0.830966
O	-1.037197	-2.365223	0.886586
O	-2.919618	-0.894973	1.354201
H	-1.943750	0.682478	2.019163
C	5.114981	-0.528203	1.698213
H	5.455327	-1.482312	1.306165
H	4.838065	-0.615099	2.745061
H	5.877382	0.234729	1.565479
S	3.691553	-0.029028	0.788629
O	3.272063	1.247290	1.327350
O	2.692031	-1.096336	1.011850
O	4.066395	0.021858	-0.620767
H	2.947903	-0.896397	-1.491989

$(IA)_2(MSA)_2(DMA)_2$:

Atoms	X	Y	Z
I	-0.773365	-0.667522	1.890054
O	-0.835212	-1.582277	3.404347
O	-0.926314	-1.889141	0.592273
O	1.113844	-0.334717	1.702172
H	1.537970	-1.102066	1.226764
I	-0.143623	2.762668	-0.660699
O	0.832237	2.919227	0.845824
O	-1.139039	1.273810	-0.305938
O	1.031872	2.186572	-1.880390
N	-0.106957	-1.994292	-1.950983
H	0.925194	-2.094808	-2.004809
C	-0.757373	-3.286307	-2.237404
H	-1.829706	-3.169917	-2.101896
H	-0.528021	-3.587128	-3.257165
H	-0.378821	-4.022918	-1.534687
C	-0.537603	-0.895825	-2.834657
H	-1.604283	-0.734752	-2.698542
H	0.014672	0.003240	-2.573199
H	-0.328925	-1.168120	-3.867074
N	3.232479	1.556519	0.667757
H	2.256246	1.895666	0.770618
C	3.833084	1.378539	2.001056
H	4.826068	0.951193	1.885316
H	3.895295	2.343924	2.497727
H	3.201824	0.705773	2.573752
C	3.961495	2.494929	-0.204989
H	4.961137	2.105686	-0.380555
H	3.419622	2.570532	-1.143942
H	4.010827	3.467722	0.278459
C	4.501735	-3.232416	-0.608887
H	4.026339	-4.204334	-0.706380
H	5.229227	-3.080929	-1.401728
H	4.969901	-3.132579	0.366342
S	3.254339	-1.990468	-0.754636
O	2.649542	-2.170869	-2.067619
O	2.306341	-2.241543	0.328376
O	3.941137	-0.711949	-0.607363
H	-2.508483	0.972437	-0.832796
C	-5.717546	-0.217000	-0.551449
H	-5.941919	0.708805	-0.030744
H	-5.985886	-0.153944	-1.602128
H	-6.219407	-1.057664	-0.079422

S	-3.990181	-0.530737	-0.433674
O	-3.430110	0.703227	-1.186963
O	-3.605192	-0.454237	0.947972
O	-3.695945	-1.720071	-1.167061
H	3.233261	0.635810	0.187547
H	-0.335026	-1.766446	-0.958764

$(IA)_3(MSA)_1(DMA)_1$:

Atoms	X	Y	Z
I	0.070600	2.011541	-1.137997
O	-0.492361	3.675426	-0.916514
O	0.595723	1.483091	0.496667
O	1.843504	2.328897	-1.811639
H	2.488649	2.010719	-1.149815
I	0.267876	-2.199968	-0.663756
O	0.468064	-0.801901	-1.745805
O	0.557663	-1.546661	0.993643
O	1.975831	-3.034185	-0.922321
H	2.696611	-2.383574	-0.786444
I	-3.246531	-0.448279	0.026224
O	-3.166219	-0.515651	1.822170
O	-2.122160	-1.778790	-0.502948
O	-2.371533	1.074426	-0.367792
H	-0.336080	0.914113	1.695409
N	-0.893623	0.853999	2.582728
H	-1.721281	0.262691	2.373972
C	-0.077686	0.240713	3.641100
H	0.850000	0.798328	3.743944
H	-0.627734	0.254355	4.579572
H	0.143745	-0.783152	3.353924
C	-1.350414	2.226101	2.868475
H	-0.483105	2.862496	3.023838
H	-1.904290	2.584098	2.004601
H	-1.985422	2.223677	3.751498
C	5.215201	-0.099532	1.626489
H	5.287047	-1.090931	2.063180
H	6.061310	0.099976	0.974046
H	5.139168	0.665733	2.393484
S	3.776858	-0.024057	0.621562
O	3.681702	1.302637	0.097718
O	3.811125	-1.101785	-0.329898
O	2.689982	-0.300839	1.678236
H	1.850751	-0.747192	1.309212

$(IA)_3(MSA)_1(DMA)_2$:

Atoms	X	Y	Z
I	2.003008	2.038126	-0.335798
O	3.074740	0.852855	0.637451
O	3.056171	3.464230	-0.420174
O	0.722168	2.484559	0.855630
H	-0.918858	2.444852	0.383330
I	2.728792	-1.307285	0.545713
O	1.943541	-0.938242	-1.057503
O	2.431711	-3.219329	0.330699
O	1.503254	-1.111842	1.829109
H	-0.224684	-1.222779	1.696293
I	-0.429251	-1.321140	-1.605300
O	-0.694633	0.202329	-0.696744
O	-2.178811	-1.510807	-2.339079
O	-0.428713	-2.611569	-0.364143
N	-1.896408	2.766986	0.213640
H	-2.563740	2.029186	0.523261
C	-2.114098	3.971779	1.031910
H	-1.405601	4.739446	0.731380
H	-3.134850	4.320257	0.895365
H	-1.947261	3.721044	2.075561
C	-2.093698	2.981634	-1.230910
H	-1.377715	3.721844	-1.582851
H	-1.946708	2.030574	-1.731944
H	-3.108184	3.332262	-1.403129
N	-1.158975	-1.088951	2.116007
H	-1.872702	-1.065613	1.370741
C	-1.466816	-2.250281	2.966093
H	-0.699370	-2.344192	3.730233
H	-2.444509	-2.109141	3.419117
H	-1.478607	-3.135246	2.336306
C	-1.148987	0.207026	2.818702
H	-0.559355	0.113946	3.727030
H	-0.674061	0.938426	2.168820
H	-2.173137	0.492531	3.046231
C	-5.947100	-0.326219	0.453885
H	-6.213316	-1.230145	-0.087111
H	-6.170913	-0.433713	1.511569
H	-6.461665	0.534896	0.036879
S	-4.208483	-0.075344	0.274824
O	-3.900004	1.139550	1.033446
O	-3.563152	-1.254444	0.830813
O	-3.959831	0.087785	-1.153338

H	-2.854251	-0.973036	-1.845030
H	1.490436	-3.344475	0.121245

Table S5. Comparison of single-point electronic energies (in kcal mol^{-1}) for selected clusters.

Clusters	ΔE (ZORA-CCSD(T))	ΔE (DLPNO-CCSD(T))	$\Delta\Delta E$
$(IA)_1(DMA)_1$	-22.81	-24.49	1.68
$(IA)_1(MSA)_1$	-24.78	-24.95	0.17
$(IA)_1(DMA)_1(MSA)_1$	-52.48	-51.50	0.98

All single-point energy calculations were carried out using cluster structures optimized at the ωB97X-D/6-311++G(3df,3pd) (for C, H, O, N, and S atoms) + aug-cc-pVTZ-PP with ECP28MDF (for I atom). In this framework, ΔE(DLPNO-CCSD(T)) denotes the electronic energy obtained at the DLPNO-CCSD(T)/aug-cc-pVTZ(-PP) level of theory, while ΔE(ZORA-CCSD(T)) refers to the electronic energy computed at the ZORA-CCSD(T)/TZVPP level of theory.

Supplementary Reference

Elm, J. and Kristensen, K.: Basis set convergence of the binding energies of strongly hydrogen-bonded atmospheric clusters, Phys. Chem. Chem. Phys., 19, 1122–1133, http://doi.org/10.1039/c6cp06851k, 2017.

Engsvang, M., Wu, H. and Elm, J.: Iodine clusters in the atmosphere I: Computational benchmark and dimer formation of oxyacids and oxides, ACS Omega, 9, 31521–31532, http://doi.org/10.1021/acsomega.4c01235, 2024.

Francl, M. M., Pietro, W. J., Hehre, W. J., Binkley, J. S., Gordon, M. S., DeFrees, D. J. and Pople, J. A.: Self-consistent molecular orbital methods. XXIII. A polarization-type basis set for second-row elements, J. Chem. Phys. , 77, 3654–3665, http://doi.org/10.1063/1.444267, 1982.

He, X.-C., Simon, M., Iyer, S., Xie, H.-B., Rörup, B., Shen, J., Finkenzeller, H., Stolzenburg, D., Zhang, R., Baccarini, A., Tham, Y. J., Wang, M., Amanatidis, S., Piedehierro, A. A., Amorim, A., Baalbaki, R., Brasseur, Z., Caudillo, L., Chu, B., Dada, L., Duplissy, J., Haddad, I. E., Flagan, R. C., Granzin, M., Hansel, A., Heinritzi, M., Hofbauer, V., Jokinen, T., Kemppainen, D., Kong, W., Krechmer, J., Kürten, A., Lamkaddam, H., Lopez, B., Ma, F., Mahfouz, N. G. A., Makhmutov, V., Manninen, H. E., Marie, G., Marten, R., Massabò, D., Mauldin, R. L., Mentler, B., Onnela, A., Petäjä, T., Pfeifer, J., Philippov, M., Ranjithkumar, A., Rissanen, M. P., Schobesberger, S., Scholz, W., Schulze, B., Surdu, M., Thakur, R. C., Tomé, A., Wagner, A. C., Wang, D., Wang, Y., Weber, S. K., Welti, A., Winkler, P. M., Zauner-Wieczorek, M., Baltensperger, U., Curtius, J., Kurtén, T., Worsnop, D. R., Volkamer, R., Lehtipalo, K., Kirkby, J., Donahue, N. M., Sipilä, M. and Kulmala, M.: Iodine oxoacids enhance nucleation of sulfuric acid particles in the atmosphere, Science, 382, 1308–1314, http://doi.org/10.1126/science.adh2526, 2023.

Kerminen, V.-M. and Kulmala, M.: Analytical formulae connecting the “real” and the “apparent” nucleation rate and the nuclei number concentration for atmospheric nucleation events, J. Aerosol Sci., 33, 609–622, http://doi.org/10.1016/s0021-8502(01)00194-x, 2002.

Khatun, M., Paul, S., Roy, S., Dey, S. and Anoop, A.: Performance of Density Functionals and Semiempirical 3c Methods for Small Gold–Thiolate Clusters, J. Phys. Chem. A, 127, 2242-2257, http://doi.org/10.1021/acs.jpca.2c07561, 2023.

Kulmala, M., Petäjä, T., Nieminen, T., Sipilä, M., Manninen, H. E., Lehtipalo, K., Dal Maso, M., Aalto, P. P., Junninen, H., Paasonen, P., Riipinen, I., Lehtinen, K. E. J., Laaksonen, A. and Kerminen, V.-M.: Measurement of the nucleation of atmospheric aerosol particles, Nat. Protoc., 7, 1651–1667, http://doi.org/10.1038/nprot.2012.091, 2012.

Lesiuk, M.: Quintic-scaling rank-reduced coupled cluster theory with single and double excitations, J. Chem. Phys. , 156, 064103, http://doi.org/10.1063/5.0071916, 2022.

Lu, T. and Chen, F.: Multiwfn: a multifunctional wavefunction analyzer, J. Comput. Chem., 33, 580–592, http://doi.org/10.1002/jcc.22885, 2012.

Ma, F., Xie, H. B., Zhang, R., Su, L., Jiang, Q., Tang, W., Chen, J., Engsvang, M., Elm, J. and He, X. C.: Enhancement of atmospheric nucleation precursors on iodic acid-induced nucleation: Predictive model and mechanism, Environ. Sci. Technol., 57, 6944–6954, http://doi.org/10.1021/acs.est.3c01034, 2023.

Peterson, K. A., Figgen, D., Goll, E., Stoll, H. and Dolg, M.: Systematically convergent basis sets with relativistic pseudopotentials. II. Small-core pseudopotentials and correlation consistent basis sets for the post-d group 16–18 elements, J. Chem. Phys. , 119, 11113–11123,

http://doi.org/10.1063/1.1622924, 2003.

Rappé, A. K., Casewit, C. J., Colwell, K. S., Goddard, W. A. and Skif, W. M.: UFF, a full periodic table force field for molecular mechanics and molecular dynamics simulations, J. Am. Chem. Soc., 114, 10024–10035, http://doi.org/10.1021/ja00051a040, 1992.

Schmitz, G. and Elm, J.: Assessment of the DLPNO binding energies of strongly noncovalent bonded atmospheric molecular clusters, ACS Omega, 5, 7601–7612, http://doi.org/10.1021/acsomega.0c00436, 2020.

Stewart, J. J.: Optimization of parameters for semiempirical methods VI: more modifications to the NDDO approximations and re-optimization of parameters, J. Mol. Model., 19, 1–32, http://doi.org/10.1007/s00894-012-1667-x, 2013.

Stewart, J. J. P.: MOPAC2016, Colorado Springs, CO (USA), http://openmopac.net/MOPAC2016.html (last access: 2022 Feb 2024), 2016.

Xia, D., Chen, J., Yu, H., Xie, H. B., Wang, Y., Wang, Z., Xu, T. and Allen, D. T.: Formation Mechanisms of Iodine-Ammonia Clusters in Polluted Coastal Areas Unveiled by Thermodynamics and Kinetic Simulations, Environ. Sci. Technol., 54, 9235–9242, http://doi.org/10.1021/acs.est.9b07476, 2020.

Yu, H., Ren, L., Huang, X., Xie, M., He, J. and Xiao, H.: Iodine speciation and size distribution in ambient aerosols at a coastal new particle formation hotspot in China, Atmos. Chem. Phys., 19, 4025–4039, http://doi.org/10.5194/acp-19-4025-2019, 2019.

Zhang, J. and Dolg, M.: ABCluster: the artificial bee colony algorithm for cluster global optimization, Phys. Chem. Chem. Phys., 17, 24173–24181, http://doi.org/10.1039/c5cp04060d, 2015.